A Review of SERF atomic magnetometer: recent advances and applications

Jundi Li, Wei Quan, Binquan Zhou, Zhuo Wang, Jixi Lu, Zhaohui Hu, Gang Liu and Jiancheng Fang

***Abstract*—This paper aims to review the technology, developments and applications of spin exchange relaxation free (SERF) atomic magnetometers. The generalized comparisons between the SERF magnetometer and the other types of weak magnetic sensors are elaborated. Further, the fundamental composition and operational principle of the SERF atomic magnetometer are elucidated. The development history and recent technological developments with respect to several aspects, including the alkali metal vapor source, atom heating method, pump and probe lasers and magnetic shielding system, are presented. The classification and respective advantages and disadvantages of these technologies are described in detail. Finally, the existing and potential applications, as well as the prospective future development trends are presented.**

***Index Terms*—SERF, atomic magnetometer, alkali metal vapor source, atom heating method, pump and probe lasers, magnetic shielding system.**

I. Introduction

The magnetic field is one of the most essential and significant physical measurement quantities, as much as inertia and gravity [1]. The accurate detection and measurement of magnetic fields, particularly the extremely weak magnetic field (below nT level), is effective for understanding the physical world [2]. There are various weak magnetic sensors, such as the fluxgate magnetometer, optically pumped magnetometer (OPM), superconducting quantum interference device (SQUID), etc., which play a prominent role in scientific research, national defense, biomedicine, and industrial production [3]–[7]. The fluxgate magnetometer, a portable solid-state device that can sense a magnetic field range of 0.1 mT to 0.1 nT, is extensively applied in geological exploration and aerospace navigation [8]. The OPM, which is the most mature and widely used atomic magnetometer, is extensively applied in anti-submarine, geological exploration of magnetic anomalies and biomedicine [4], [9]. In 2002, the Polatomic company developed a product with a high sensitivity of 50 fT/Hz$^{1/2}$ [10]. In the past few decades, the low temperature SQUID has been the most sensitive low frequency magnetic detector, demonstrating a superhigh sensitivity of 1 fT/Hz$^{1/2}$ [11]–[13]. Benefiting from its high sensitivity, SQUID is widely used in many areas, especially in biology, such as magnetoencephalography (MEG), magnetogastrography (MGG) and magnetic resonance imaging (MRI) [14]. However, before operation, SQUIDs need expensive liquid helium to be maintained in a superconducting state, resulting in increased size and high maintenance costs. Besides, some special magnetic measurement cases, such as the analysis of the chemical composition and structure, brain science, and fundamental physical research, urgently require more sensitive and miniaturized magnetometers [15]–[17].

With the development of quantum science and manipulation technology, the SERF atomic magnetometer was first proposed by the Romalis lab at Princeton university in 2002 [13]. Since then it has been receiving considerable attention and extensive researches. The SERF magnetometer is a new type of alkali metal atomic magnetometer, which operates in the SERF regime and belongs to the optical magnetometer category. It also called all-optical atomic magnetometer due to the commonly adopted pump-probe full optical structure [18]. Unlike the traditional atomic magnetometer, the sensitivity of the SERF magnetometer is no longer affected by spin exchange relaxation. After years of development, SERF magnetometers have surpassed the SQUID and are currently the most sensitive sensors, achieving an ultrahigh sensitivity of 0.16 fT/Hz$^{1/2}$ in a gradiometer arrangement [19]. Using these SERF magnetometers, it can not only achieve a higher sensitivity, but also possess the advantages of non-cryogenic operation, high spatial resolution and miniaturization. Therefore, the SERF magnetometers will be widely applied in some fields that the SQUIDs are not competent, especially in biological magnetism [20]. The SERF regime can be realized under conditions of high atomic number density, low magnetic field (less than 10 nT) and efficient optical pumping.

II. Fundamental composition and operate principle

The SERF atomic magnetometer is an ultra-high sensitive atomic magnetometer operating in the SERF regime. For conventional atomic magnetometer, the sensitivity is often limited by the spin exchange collision relaxation and can not be further improved. However, the SERF atomic magnetometer breaks through this limitation. The spin exchange relaxation mechanism is closed and no longer affects the sensitivity, when the spin exchange rate is considerably greater than the Larmor precession frequency. In order to increase the spin exchange rate and decrease the Larmor precession frequency simultaneously, high atomic number density and extremely low

Manuscript received April 18, 2018; revised June 24, 2018; accepted July 28, 2018. This work was supported by the 863 Plan of China under Grant Nos.2014AA123401, the Key Programs of the National Science Foundation of China under Grant Nos.2016YFB051600 and the National Natural Science Foundation of China under Grant Nos.61227902. Corresponding author: Jundi Li and Wei Quan*(e-mail: quanwei@buaa.edu.cn, lijundi-a@163.com).

The authors are with the School of Instrumentation Science and Opto-electronics Engineering, Beijing University of Aeronautics and Astronautics, Beijing 100191, China, and also with China Science and Technology on Inertial Laboratory, Beijing University of Aeronautics and Astronautics, Beijing 100191, China.

This article has been accepted for publication in a future issue of this journal, but has not been fully edited. Content may change prior to final publication. Citation information: DOI 10.1109/JSEN.2018.2863707, IEEE Sensors Journal

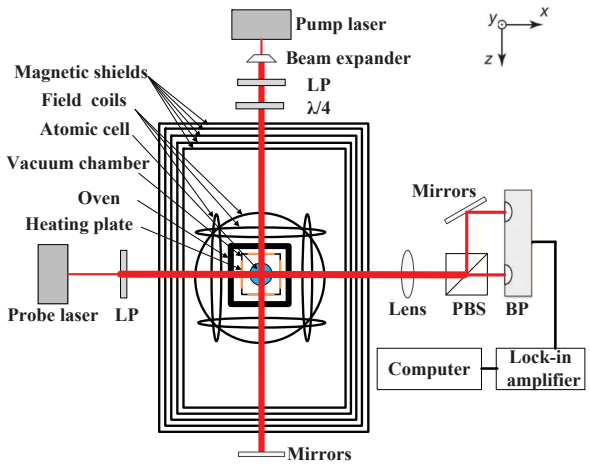

Fig. 1. Essential composition of an atomic magnetometer. (LP:linear polarizer; PBS:polarizing beam splitter; BP:balanced detector).

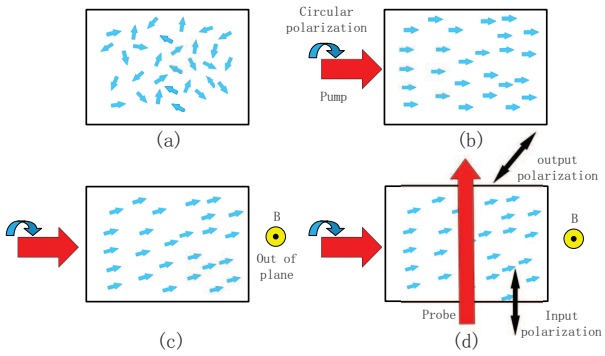

Fig. 2. Operating principle of an atomic magnetometer. (a) Random atomic spin in the natural state, (b) Spin polarization by optical pumping using circularly polarized light, (c) Spin precession with a magnetic field, and (d) Detection of optical rotation angle using linear polarized light.

magnetic field are necessary, which can be realized by the heating system and magnetic shielding system, respectively. The composition and fundamental principle of SERF atomic magnetometer are demonstrated as follows.

A. Elementary composition

The essential composition of a typical atomic magnetometer is depicted in Fig.1, it mainly includes a core atomic glass cell, square oven with nonmagnetic electric heating plates, small vacuum chamber, magnetic shielding system, pumping and probing optical system, data acquisition and processing system, and other electronic auxiliary equipment. The atomic cell, with a diameter in the order of centimeter level, contains a droplet of alkali metal atoms, several atm of inert gas ^{4}He for reducing wall collision relaxation and quenching gas N_2 for eliminating the radiation capture effect. Although various alkali atoms are available, K, Rb and Cs are generally used [21]. A inert buffer gas, such as He or Xe, is often utilized. The electric heating plates are amounted on the six surfaces of the oven, which is placed in a small vacuum cavity. A titanium wire is wound symmetrically to eliminate the magnetic field generated by the current. The nonmagnetic electric heating system provides a sufficiently high atomic number density of approximately ($10^{13}\sim 10^{15}$) [22], ensuring SERF regime realization. Outside the small vacuum chamber, successive three axis quadrature Helmholtz coils and a multilayer shield are utilized to attenuate the external stray magnetic field to less than 10nT. The optical system, including the pump and probe optical path, which generally adopts the orthogonal configuration to achieve the highest sensitivity, is the core of the whole system. Pumping and detecting lasers are used for driving the atomic spin on a fixed axis and detecting the atom spin direction, respectively. A typical pump optical path includes a beam expander, a linear polarizer, a quarter waveplate and a reflector, whereas typical probe optical path includes a focus lens, a linear polarizer, a quarter waveplate and a reflector, a polarizing beam splitter (PBS), a prism and a balanced detector.

B. Fundamental principle and theory

The magnetic momentum originating from atomic spin executes a Larmor precession, if it is influenced by an external magnetic field. Thus, the magnetic field intensity can be acquired, based on the atomic spin effect. The relationship between the magnetic field and precession frequency can be determined by

$$\omega = \gamma * |B| \tag{1}$$

where ω is the Larmor precession frequency, γ is the alkali atom gyromagnetic ratio, and the absolute value of B is the amplitude of the applied magnetic field. As the spin angular momentum of a single atom is minimal, an atomic ensemble is necessary and is utilized commonly [12].

The operating principle of an atomic magnetometer is depicted in Fig.2. In the natural state, the spin direction of the atomic ensemble is random. A resonant circularly polarized light tuned in the D1 transition line of the alkali atoms polarizes the atomic ensemble, causing them to spin along the same pumping direction. When a measured magnetic field is applied to the polarized atomic assemble, it undergoes Larmor precession, which further changes the optical property of the alkali atoms. The linearly polarized detection light is tuned off-resonant in the D2 line of alkali atoms. After it propagates through the cell, the polarization plane of the probe beam deviates by a small angle from the pumping direction. Therefore, the applied magnetic field can be determined by measuring the rotation angle. Customarily, we specify the pump direction as the Z–axis, probe light direction as the X–axis and the applied magnetic field as the Y–axis. The mechanism of atomic spin evolution with a laser and magnetic field can be integrally described by the the density matrix equation based on quantum mechanics. The density matrix equation is depicted below:

$$\begin{aligned}\frac{d\rho}{dt} &= D\nabla^2\rho + A\frac{[\mathbf{I}\cdot\mathbf{S},\rho]}{i\hbar} + g_s\mu_B\frac{[B\cdot S,\rho]}{i\hbar} + \frac{\varphi-\rho}{T_{SD}} \\ &+ \frac{\varphi(1+4\langle\mathbf{S}\rangle\cdot\mathbf{S})-\rho}{T_{SE}} + R_{OP}[\varphi(1+2s\cdot\mathbf{S})]\end{aligned} \tag{2}$$

where $\varphi = \rho/4 + \mathbf{S}\cdot\rho\mathbf{S}$ is the nuclear part of the density matrix. T_{SE} is the spin exchange relaxation time. T_{SE} is the spin

destruction relaxation time. R_{op} is the relaxation rate induced by the pump beam. $\mathbf{B}$ is the magnetic field vector perceived by the atomic ensemble. $\mathbf{S}$ is the spin vector of the alkali atoms.

The density matrix equation is approximately linearized to the classical Bloch equation due to the small magnetic field and rotation angle [12], [21].

$$\frac{d}{dt}\mathbf{S} = \frac{1}{q}[\gamma(\mathbf{B} + B_{LS}\hat{z}) \times \mathbf{S} + R_{op}(\frac{1}{2}\mathbf{s}\hat{z} - \mathbf{S}) - R_{tot}\mathbf{S}] \quad (3)$$

where q is the slowing factor caused by nuclear spin. B_{LS} is the virtual magnetic field resulting from the optical frequency shift. R_{tot} is the total spin relaxation rate. $\mathbf{s}$ is the optical pumping vector, whose direction reveals the pumping orientation while the size demonstrates the circular polarization degree. When a circularly polarized light is used for pumping light, the value of $\mathbf{s}$ can be considered as unity.

Quasi-static spin evolution is acquired by making both sides of the equation zero, the obtained solution of the spin projection component in the X–direction, S_x, is depicted in (4), as follows. Defining the parameter $\beta = R_{op} + R_{tot}/\gamma$, then the S_x can be deduced as

$$S_x = \frac{R_{op}}{2\gamma\beta}\frac{\beta B_y + B_x(B_z + B_{LS})}{(\beta^2 + {B_x}^2 + {B_y}^2 + (B_z + B_{LS})^2)} \quad (4)$$

When the residual magnetism in the X, Y and Z directions are well compensated to zero and the effect of optical frequency shift is negligible, the approximate conditions can be regarded as $B_x = 0$, $B_y = 0$, and $(B_z + B_{LS}) = 0$. Only a small measured field, B_{ey}, in the Y–direction is applied, which satisfies $\gamma B_{ey} \ll (R_{op} + R_{tot})$; S_x can be simplified as

$$S_x = \frac{R_{op}}{2(R_{op} + R_{tot})}\frac{\gamma B_{ey}}{(R_{op} + R_{tot})} \quad (5)$$

Parameter, $S_0 = \frac{R_{op}}{2(R_{op}+R_{tot})}$, and scale factor, $K = \frac{\gamma}{R_{op}+R_{tot}}$, are introduced. Thus, the following formula is obtained:

$$S_x = S_0 K B_{ey} \quad (6)$$

where S_0 is the spin projection component without an external magnetic field, and K represents the calibration coefficient in the external magnetic field.

When linear polarized light in the D2 line of alkali atoms propagates through the cell, the total polarization angle can be expressed as:

$$\theta = \frac{\pi}{2}\mathrm{nl}\gamma_{\mathrm{c}}\mathrm{S_x}\mathrm{f_{D2}}\{\mathrm{I}m[V(v - v_{D2})]\} \quad (7)$$

where n is the atomic number density, which is closely related to the heating temperature. l is the optical length of the detecting laser in the atomic cell. $\mathrm{f_{D2}}$ is the oscillating factor. $\mathrm{I}m[V(v - v_{D2})]$ represents the imaginary part of the Voigt profile, which can be approximately replaced by the imaginary part of the Lorentz function.

When the Doppler broadening is considerably greater than the sum of the natural lifetime and pressure broadening [12]. Thus, (7) is further simplified to (8)

$$\theta = \frac{1}{2}\mathrm{nl}\gamma_{\mathrm{e}}\mathrm{c}\mathrm{P_x}\mathrm{f_{D2}}\frac{v - v_{D2}}{(v - v_{D2})^2 - (\Gamma/2)^2} \quad (8)$$

where v_{D2} is the resonant frequency and Γ is the full width at half maximum.

III. Research History and Current Developments

In 1957, Dehmelt *et al.* [23] originally proposed the observation of alkali atom spin precession for determining the magnetic field strength. This idea was experimentally verified by Bell and Bloom *et al.* in the same year [24]. In 1973, W.Happer and H.Tang *et al.* [25], at Columbia university, discovered that spin exchange relaxation is suppressed when the spin exchange rate is considerably greater than the Larmor precession frequency, here, a 200 Hz magnetic resonance linewidth was observed for an atomic number density of 10^{14}. Subsequently, a theoretical explanation for this phenomenon was presented [26]. In 2002 in Washington, J.C.Allred *et al.* [13] first proposed the SERF magnetometer term, where the spin exchange relaxation mechanism was closed and no longer affected the sensitivity. The current developments in SERF magnetometers are described in detail, with respect to several areas, as follows.

A. Alkali metal vapor source

A alkali metal gas chamber is the sensitive core of ultra-high sensitive magnetic fields and inertial measurements. The atomic source species determines the measurement sensitivity limit. Here, we discuss in detail the influence on the sensitivity by two entities: single and hybrid alkali atoms.

SERF regime realization generally requires highly saturated vapor density, hence, an operating temperature of more than 373 K is necessary and is utilized. For the SERF atomic magnetometer, in addition to the high heating temperature required, the minimum temperature gradient is also necessary for more uniform atomic polarization. The degree of heating depends on the employed alkali atoms. Under the same density requirement, K should be heated to the highest temperature, followed by Rb and Cs, because the saturation vapor pressure of K, Rb and Cs increase accordingly. However, the sensitivity based on K atoms is the highest, followed by Rb and Cs [27]. In 2003 and 2010, at Princeton university, K SERF magnetometers were heated to 453 K and 473 K at cell volumes of 0.3 cm^3 and 0.45cm^3 each, achieving sensitivities of 0.54 fT/$\mathrm{Hz}^{1/2}$ [1] and 0.16 fT/$\mathrm{Hz}^{1/2}$ [19], respectively. In 2014, at the Korea Research Institute of Standards and Science (KRISS), a multichannel K SERF magnetometer was heated to 473 K, achieving a gradient sensitivity of 4 fT/$\mathrm{Hz}^{1/2}$ [28]. In 2010, at the Sandia National Laboratory, an Rb SERF magnetometer was heated to 463 K, achieving a sensitivity of 5 fT/$\mathrm{Hz}^{1/2}$ [29]. In 2007 and 2010, at the National Institute of Standards and Technology (NIST), an Rb SERF magnetometer were heated to 425 K and 473 K, achieving a sensitivity of 70 fT/$\mathrm{Hz}^{1/2}$ [30] and 5 fT/$\mathrm{Hz}^{1/2}$ [31], respectively. In 2006 and 2012, at the university of Wisconsin Madison, Rb SERF magnetometers were heated to 461 K and 413∼443 K, achieving sensitivities of 60 fT/$\mathrm{Hz}^{1/2}$ [32] and 6∼11 fT/$\mathrm{Hz}^{1/2}$ [20], respectively. In 2008, M. P. Ledbetter described a Cs SERF magnetometer, which was heated only to 376 K, achieving a sensitivity of 40 fT/$\mathrm{Hz}^{1/2}$ [33]. An estimated theoretical sensitivity in the order of 0.2 fT/$\mathrm{Hz}^{1/2}$ should be achievable with a volume of 1 cm^3. In 2015, Beihang university had achieved a sensitivity of 55 fT/$\mathrm{Hz}^{1/2}$ in a

single channel with a heating temperature of 358 K [34], for the Cs SERF magnetometer. The Cs atomic magnetometer is advantageous to apply in the low temperature field, such as microfluidic NMR [35].

In addition to the single alkali atomic magnetometer, there is a hybrid pumping atomic magnetometer, whose cell contains two or more than two types of alkali atoms, such as K-Rb and K-Cs. Different from the single alkali atomic magnetometer, the hybrid pumping magnetometer utilizes spin exchange optical pumping (SEOP) to achieve electron spin polarization [36]. In order to state the operating principle of the SEOP, we introduce symbols A and B as substitutes for the two types of atoms. Initially, the pumping light polarizes atom A; the polarized atom A then repolarizes atom B. This has the advantage of reduced optical depth (OD) and uniform spin polarization, hence, it is more suitable for brain science research. In 2010, the hybrid pumping atomic magnetometer was first demonstrated by professor M.V.Romails *et al.* [37] at Princeton university. It was occasionally found that the sensitivity of pumping the K atom with a trace contamination of Rb had a polarizability that was 4.5 times higher than directly pumping K in the absence of N_2. This discovery promoted hybrid pumping research. In 2011, Professor Yosuke Ito *et al.* [38] at Kyoto university in Japan commenced research on hybrid pumping. They mainly concentrated on the K-Rb hybrid pumping and studied four different configurations (pump K and detect Rb, pump Rb and detect Rb, pump Rb and detect K, pump K and detect K), finally determining that pumping K and probing Rb was the most sensitive configuration, which achieved an ultrahigh sensitivity up to 30 fT/Hz$^{1/2}$. In 2012, Professor Yosuke Ito *et al.* [39] utilized dense Rb as detection atoms and achieved a lower linewidth and sensitivity of approximately 100 fT/Hz$^{1/2}$ at 10 Hz, compared to direct Rb pumping. Besides, they summarized and concluded that the pumping efficiency of K-Rb hybrid atoms was greater than single K atoms [40]. In 2013, Kyoto university theoretically studied the properties of the hybrid magnetometer using the rate equation. An optimum density ratio of 200 for K and Rb was proved to obtain the best sensitivity [41]. In 2014, Beihang university had achieved a sensitivity of 5 fT/Hz$^{1/2}$ in a gradiometer arrangement with a heating temperature of 468 K [42], for the K-Rb SERF magnetometer.

To maximize the output signals and improve spatial homogeneity, in 2016, Kyoto university researched the K-Rb Bloch equation, considering the effect of the spatial distribution of spin polarization. Finally, an optimum density ratio of 400 for K and Rb was determined and the density of K was 3×10^{19} m^{-3} [43]. K-Cs and Cs-Rb hybrid pumping magnetometers are rarely studied. The heat temperature and sensitivity of different alkali metal atoms are listed in Table I, in addition.

B. Heating operation of alkali metal atoms

To obtain sufficiently high atomic number density, a heating operation is commonly necessary and utilized. There are several heating methods, including hot airflow heating, intermittent electrical heating, high frequency nonmagnetic electrical heating and laser heating. During the early stage of atomic magnetometer research, hot airflow heating was widely employed by major research institutes, such as Princeton university [1], UC Berkeley [33], Sandia National Laboratory [44], etc. The advantage of hot airflow heating is that magnetic noise is not introduced throughout the heating process, and its structure is simple and easy to implement. However, there are several shortcomings: it is bulky and difficult to miniaturize due to the use of air compressors, the sensitivity is easily influenced by serious low frequency interference from thermal gas disturbances, and the temperature control precision is low. Hence, intermittent electrical heating was proposed, which refers to alternate operation at certain frequency [31]. The magnetic measurement performance is maintained during the interval, because the intermittent electrical heating interval is short. Thus, the interference caused by electric heating can be negligible because the change in the temperature of the cell is negligible. Although this method is simple in structure and easy to implement, continuous measurement is impossible and the temperature control accuracy is limited. In order to avoid the introduction of additional magnetic noise, nonmagnetic electrical heating was proposed [19], [45], [46], which employs a double winding symmetry structure to reduce the magnetic noise generated by electric wires. Further, low frequency magnetic noise should be reduced by modulating the drive current to a specific frequency (generally tens to hundreds of kHz). The advantages are less low frequency noise and high temperature control accuracy. In addition, there is the laser irradiation heating method, which adopts a laser far from the alkali atom working spectrum to avoid the influence of the laser on optical pumping and detection [17], [47]. The advantage of laser heating is that the structure is simple and easy to integrate. However, the drawback is that it is only suitable for the MEMS atomic magnetometer due to less laser power (only mW).

C. Pump and probe light system

a) Laser frequency and power stabilization: The essence of optical pumping is the atomic energy level transition and the change of the atomic layout number. Traditionally, pumping light sources utilized ordinary lamps, which limited the sensitivity from further improvement. The development in technology, particularly the emergence of the laser as a pumping light source, enabled spectacular enhancement in the sensitivity. In order to improve the efficiency of atomic spin polarization, we need to select and maintain the frequency of the driving laser at a value, where the photon absorption cross section is maximum. Simultaneously, to reduce the effect of light shift [48], [49], we need to select and maintain the frequency at a value, where the light shift is zero. The laser frequency and power fluctuation have significant influence on the sensitivity of the atomic magnetometer. The methods of laser power and long-term frequency stabilization are necessary and should be manipulated. The general frequency stabilization methods include laser temperature and current source control and the wavemeter method, while the high precision methods mainly include saturated absorption spectroscopy [50], polarization spectrum frequency stabilization [51]–[53], dichroic atomic

TABLE I
HEAT TEMPERATURE AND SENSITIVITY OF DIFFERENT ALKALI METAL ATOMS

Time	Research institutions	Atomic source	Heat temperature(kelvin units)	Sensitivity($fT/Hz^{1/2}$)	Reference
2003	Princeton university	K	453	0.54	[1]
2010	Princeton university	K	473	0.16	[19]
2014	KRISS	K	473	4	[28]
2010	Sandia National Laboratory	Rb	463	5	[29]
2007	NIST	Rb	425	70	[30]
2010	NIST	Rb	473	5	[31]
2006	University of Wisconsin Madison	Rb	461	60	[32]
2012	University of Wisconsin Madison	Rb	413-443	6-11	[20]
2008	UC Berkeley	Cs	376	40	[33]
2015	Beihang university	Cs	358	55	[34]
2014	Beihang university	K-Rb	468	5	[42]
2011	Kyoto university	K-Rb	450	30	[38]

TABLE II
ADVANTAGES AND DISADVANTAGES OF THE FREQUENCY STABILIZED METHODS

Frequency stabilized methods	Advantages	Disadvantages
Laser source control	no additional optical path	open Loop control
Wavemeter method	large frequency range; no additional optical path	large volume
Saturated absorption	high precision; simple optical path	need modulation
Polarization spectrum	simple optical path; high accuracy	affected by magnetic field
DAVLL detuning	wide capture range	affected by skewed magnetic field and temperature
Faraday method	wide detuning range	affected by magnetic field and temperature
DFDL	requires no modulation	small capture range

vapor laser lock (DAVLL) [54], [55], the Faraday method [56], [57], Doppler free dichroic lock (DFDL) [58], etc. With these high precision methods, a frequency stability of several kHz per hour and a detuning range of approximately 2 GHz, within the resonant absorption peaks, can be achieved. The laser temperature and current control method does not require additional optical paths, however, it involves open loop control. The advantage of the wavemeter method is that it does not requires additional light paths and its frequency range is wide, however, the volume is large due to the wavemeter. The advantages of saturated absorption include high precision, and a stable and simple light paths; furthermore, it is not affected by environmental temperature and magnetic field, but it requires modulation and phase sensitive detection. In polarization spectrum frequency stabilization, although the optical path is simple and the accuracy high, it is easily affected by the environmental magnetic field. Although the DAVLL has a wide capture range, it is easily affected by a skewed magnetic field and ambient temperature. The Faraday method has a wide detuning range and frequency stabilization point; however, it is easily affected by the temperature and magnetic field. The DFDL does not require modulation of the laser frequency; however, it has a smaller capture range in comparison with the linear doppler-broadened dichroic lock. The advantages and disadvantages of the above methods are listed in Table II, in addition.

There are generally two ways of improving the laser power stability. The first involves the direct change of the injection current of the laser diodes and temperature control. The power stability precision of this method is in the order of 10^{-2}. However, it can not inhibit the power fluctuation caused by external factors; thus, the second method is proposed, using external optical modulation devices, such as acoustic optical modulation devices [59], [60] electro-optic modulators [61], liquid crystal variable retarders (LCVR) [62] etc.; the stability accuracy can be up to 10^{-4}, through negative feedback inhibition of the laser power fluctuation. The LCVR [62] utilizes liquid crystal to control a wave plate with birefringence characteristics and is compact with a and low working voltage, which is advantageous for miniaturization.

The detection of a weak deflection angle signal is mainly realized by two methods: directional circular diachronic and circular birefringence [13]. The Birefringence, which is a commonly employed method, utilizes the difference in the refractive indices between the left-handed and right-handed circular polarized light to detect the deflection angle [12]. Birefringence includes the differential polarization method [63], [64], Faraday modulation [1], [13], [65], the photoelastic modulator (PEM) [45], [66], electro-optic modulator (EOM) [67] etc. The differential polarization detection optical path mainly includes a PBS and photodetector. After it passes through the cell, the linear polarization probe light is divided into two orthogonal components by the PBS; the light intensities of the two components are then received by the photodetector. Thus, the deflection angle of the probe light can be obtained by calculating the difference between the two components. This method can eliminate common mode noise; however, the low frequency signal-noise ratio is

poor because there is no modulation. In order to solve this problem, modulation detection was proposed to remarkably surpass low frequency noise by modulating the low frequency optical signal to a high frequency. Prior to 2009, the Romalis group generally utilized the Faraday and difference detection methods to obtain the optical rotation angle, and in 2009, they presented PEM modulation to replace Faraday modulation and difference detection [66]. Although Faraday modulation was replaced later, differential detection continues to have certain applications. Faraday modulation modulates the phase of the input light with time, based on the magneto-optic effect, and measures the modulated beam intensity. The measurement accuracy is nearly unaffected by the vibrations of the frequency, and intensity of the laser source and optical devices because the low frequency noise has negligible impact on the small rotation signal. The disadvantage is the large volume, which is unsuitable for miniaturization. The PEM modulates the input light phase with time, based on the photo-elastic effect. This modulation is characterized by not only a low driving voltage and power consumption, but also a negligible temperature influence, and it does not emit light. The EOM modulates the input light phase with time, based on the electro-optic effect. It is well suited for system integration and miniaturization because the modulator is compact.

b) Pump and probe light configuration: Besides laser frequency stabilization, a reasonable light path layout is critical for the sensitivity. The orthogonal pump and probe beam is an optimal configuration for achieving high sensitivity. However, the near parallel and small angle configurations are more appropriate for miniaturization. In 2016, Todor Karaulanovl *et al.*, at the Los Alamos National Laboratory in USA, proposed a small angle (near parallel) beam configuration [68], which demonstrated a sensitivity of 10 fT/Hz$^{1/2}$ within a frequency range of 10$\sim$100 Hz. Besides, the single beam configuration, suitable for multichannel biomagnetic signal detection, was also presented, in this time period. The single beam configuration generally utilizes either elliptically or circularly polarized light to realize pumping and detection simultaneously; it is easy to miniaturize and has relatively high sensitivity. In 2009, V. Shah *et al.*, at Princeton university, realized the SERF state with single beam fiber-coupled elliptically polarized light, achieving a sensitivity of 7 fT/Hz$^{1/2}$ with an 5$\times$5$\times$5 mm Rb cell [22]. In 2009, Dr Li *et al.* also adopted a single beam configuration and realized a sensitivity of 0.5 pT/Hz$^{1/2}$ with an Rb atomic cell [69]. In 2016, Dr Huang *et al.*, at Beihang university, researched the three–axis vector measurement of a single beam magnetometer with a Cs atomic cell [70], and achieved a demodulation sensitivity of 300 fT/Hz$^{1/2}$ in the X and Y axes, simultaneously, and a sensitivity of 3 pT/Hz$^{1/2}$ in the Z axis. Moreover, a dual-beam difference probe was demonstrated to cancel the common mode nonmagnetic technical noises [71], indicating that the expected practical and fundamental sensitivities are comparable to the orthogonal geometry.

Unlike the traditional magnetometer, the sensitivity of a SERF magnetometer is defined as the linewidth, ΔB, divided by the signal-to-noise ratio; S/N, δB=ΔB/(S/N) [12]. To obtain high sensitivity, it is effective to enhance the signal intensity and restrain noise as far as possible. In order to increase the signal output, in 2011, the Romails group studied the multi-pass cell optical rotation angle, which can be accumulated to exceed 100 rad because the optical path is prolonged by the multiple-pass atomic cell [72]. In 2013, using the multi-pass cell, a scalar atomic magnetometer had realized a sensitivity in the subfemtotesla level [64]. The multi-pass method can play an important role in increasing the S/N of microcells and can be adopted in nuclear magnetic resonance gyroscope (NMRG) [73].

D. Magnetic shielding system

A weak magnetic environment is one of the prerequisites for the implementation of the SERF state. Therefore, an efficient magnetic shielding system is indispensable for attenuating the external stray magnetic field to less than 10nT or ideally zero [18]. In addition to the extremely weak remanence, the magnetic field gradient and low magnetic noise are required to be as small as possible for ultra-high sensitivity. The shielding system mainly includes an active magnetic compensation system and a passive magnetic screen system [74].

For the SERF atomic magnetometer, the active magnetic compensation system generally involves a set of three axis quadrature Helmholtz coils mounted within a shield to further attenuate the remanence and provide a calibrating magnetic field. In addition to compensation coils, there are several different magnetic field compensation methods. In 2004, S.J.Seltzer *et al.*, at Princeton university, proposed cross modulation [63]; the magnetic fields are modulated by applying sinusoidal fields at different frequencies in the X and Z directions, respectively. The magnetic field in the Y direction is obtained by detecting the DC term. The magnetic field components in the X and Z directions are detected by a lock-in amplifier at a different modulated frequency. The advantage is that it can realize three axis vector measurement while the shortcomings are a narrow bandwidth and the strict requirements of quasi-static conditions. In 2006, Zhimin Lia *et al.*, at Wisconsin university, proposed parametric modulation [32]; the modulated field in the Z direction is utilized, and the primary frequency and second harmonic frequency signals are measured simultaneously by a lock-in amplifier, corresponding to the field components in the X and Y directions, respectively. This method has large bandwidth and can restrain light vibration and hot gas flow noise. However, only biaxial vector measurement can be obtained. In 2008, Ledbetter *et al.*, at Berkeley university in California, proposed in situ magnetic compensation [33]; a sinusoidal modulated field is applied in the X-axis, and the magnetic field in the Z-axis is obtained by a lock-in amplifier. Similarly, the magnetic field in the X-axis can be acquired by imposing a modulated magnetic signal in the Z-axis. The advantage is high compensation accuracy and the disadvantage is that only serial compensation for the two directions is possible. In 2012, Dr Qin *et al.*, at Beihang university, proposed a compensation method suitable for large magnetic environment [75]; although the structure is simple, the compensation accuracy is not high. In 2014, Dr Wang *et al.*, at Beihang university, proposed sequential magnetic

compensation considering the probe optical pumping effect [76], which demonstrated better long-term performance.

A passive magnetic shield commonly refers to a multi-layer shield composed of high permeability material such as permalloy and mumetal, which provides a high shielding factor of approximately 10^6; however, it causes magnetic noise. The magnetic noise of the high permeability shield and the conducting objects, with a simple geometry arising from the Johnson current, can be computed by a formula [77]. With the increase in magnetic measurement sensitivity, the magnetic noise from the shield itself becomes nonnegligible and restricts further improvement in the sensitivity. Atomic magnetometer noise can be mainly divided into three categories: quantum noise, magnetic noise and technical noise. The quantum noise is determined by the indeterminacy principle in quantum mechanics, and consists of spin projection noise, photon shot noise and light shift virtual magnetic noise. Currently, compared to the other two noises, the magnetic noise is the key factor that limits sensitivity enhancement. In order to reduce the magnetic noise, in 2007, a low noise MnZn ferrite was utilized as the innermost layer shield, which improved the shield performance by an order of magnitude [45]. A low noise magnetic shield has a certain magnetic permeability, which can be used to shield the external magnetic field to small remanence. On the other hand, the magnetic noise produced by itself is very weak. Low noise magnetic shields are expected to be the research focus and trend in ultrahigh sensitivity magnetic field and inertial measurement in future.

IV. Application and future prospects

c) MEG application: Since the appearance of SERF magnetometers, they have been used in various areas, such as the fundamental science research on EDM [78], exotic spin-dependent interactions [79], and paleomagnetism [19]. SERF magnetometers can measure the magnetic field and inertia, simultaneously [80]. Both single and hybrid atomic magnetometers consider only the electron spins and ignore the nucleon spins. However, when the electron and nucleon spins are both considered, a comagnetometer emerges, which is mainly formed by the polarized electrons of alkali atoms and the hyperpolarization nuclei of inert gases, such as Cs-^{129}Xe [12], K-^{3}He [81], K-Rb-^{21}Ne [82], ^{3}He-^{129}Xe [83], etc. The comagnetometer was based on the magnetometer and further developed into the atomic gyroscope. Comagnetometers were often used for ultrahigh sensitive rotation sensing because they were no longer sensitive to the static magnetic field. Besides, they had been used beyond the standard models of physics such as searching for CPT violation [84], Lorentz symmetries [85], and spin-spin interaction force [86].

The most potential and emphatic application is MEG. MEG research using SERF atomic magnetometers are described in detail below. In 2006, H. Xia *et al.* [87] at Princeton university, detected and mapped the brain magnetic fields evoked by auditory stimulation using a K SERF magnetometer, whose gradient sensitivity was equal to 3.5 fT/Hz$^{1/2}$; six–channel brain signals were obtained using a linear photodetector array. In 2014, Kiwoong Kim *et al.* [28], at the Korea Research Institute of Standards and Science, successfully localized the auditory evoked fields from human brain activity using a multi-channel K SERF magnetometer with a gradient sensitivity of 4 fT/Hz$^{1/2}$. In 2010, Cort Johnson *et al.* [29], at Sandia National Laboratories, recorded the signals from a median nerve and auditory stimulation using a fibercoupled multichannel Rb SERF magnetometer. Although pumping and detection are coaxial, the parameters of the pumping and detecting beam can be adjusted and optimized by the unique two-color pump/probe technique, respectively. Further, Cort Johnson and P. D. D. Schwindt *et al.* [88], at Sandia National Laboratories and the university of New Mexico, utilized the magnetic labeling method to determine the number of cells in a tumor. Further, in 2013 and 2016, Sandia National Laboratories implemented a multi-channel multi-sensor SERF magnetometer to measure MEG signals [89], [90].

d) future prospects: Currently, the fundamental sensitivity limits of SERF magnetometers have not yet been attained; hence, improvement in the sensitivity can be expected in future. In order to acquire the theoretical sensitivity, the research keynote should first involve the design of a low noise ferrite magnetic shield to decrease the magnetic noise further. Next, the closed loop manipulation of atomic spin ensembles should be realized and utilized for reducing signal noises. Besides, miniaturization is also important for MEG research [16]. Considerable effort must be applied to chip-level SERF magnetometers, based on MEMS technology.

References

[1] I. K. Kominis, T. W. Kornack, J. C. Allred, and M. V. Romalis, "A subfemtotesla multichannel atomic magnetometer," *Nature*, vol. 422, no. 6932, pp. 596–599, 2003.
[2] R. Fitzgerald, "New atomic magnetometer achieves subfemtotesla sensitivity," *Physics Today*, vol. 56, no. 7, pp. 21–24, 2003.
[3] P. Ripka and M. Janosek, "Advances in magnetic field sensors," *IEEE Sensors Journal*, vol. 10, no. 6, pp. 1108–1116, 2010.
[4] E. Boto, S. S. Meyer, V. Shah, O. Alem, S. Knappe, P. Kruger, T. M. Fromhold, M. Lim, P. M. Glover, P. G. Morris *et al.*, "A new generation of magnetoencephalography: Room temperature measurements using optically-pumped magnetometers," *NeuroImage*, vol. 149, pp. 404–414, 2017.
[5] E. Alexandrov, "Recent progress in optically pumped magnetometers," *Physica Scripta*, vol. 2003, no. T105, p. 27, 2003.
[6] K. Kim, "Ultra-sensitive optical atomic magnetometers and their applications," in *Advances in Optical and Photonic Devices*, 1st ed. Croatia: InTech, 2010, ch. 17, pp. 330–352.
[7] R. Fagaly, "Superconducting quantum interference device instruments and applications," *Review of scientific instruments*, vol. 77, no. 10, p. 101101, 2006.
[8] M. Djamal, E. Sanjaya, Yulkifli, and Ramli, "Development of fluxgate sensors and its applications," in *International Conference on Instrumentation, Communications, Information Technology, and Biomedical Engineering*, 2011, pp. 421–426.
[9] S. Morales, M. Corsi, W. Fourcault, F. Bertrand, G. Cauffet, C. Gobbo, F. Alcouffe, F. Lenouvel, M. Le Prado, F. Berger *et al.*, "Magnetocardiography measurements with 4he vector optically pumped magnetometers at room temperature," *Physics in Medicine & Biology*, vol. 62, no. 18, p. 7267, 2017.
[10] D. Overway, T. Clem, J. Bono, and J. Purpura, "Evaluation of the polatomic P-2000 laser pumped He-4 magnetometer/gradiometer," in *Oceans*, vol. 2, 2002, pp. 952–960.
[11] Z. Li, "Development of a parametrically modulated serf magnetometer," Ph.D.dissertation,Dept.Medical Physics, University of Wisconsin-Madison, Madison,Wisconsin, 2006.
[12] S. J. Seltzer, "Developments in alkali-metal atomic magnetometry," Ph.D.dissertation,Dept.physics, Princeton University, Princeton,New Jersey, 2008.

[13] J. C. Allred, R. N. Lyman, T. W. Kornack, and M. V. Romalis, "High-sensitivity atomic magnetometer unaffected by spin-exchange relaxation." *Physical Review Letters*, vol. 89, no. 13, p. 130801, 2002.

[14] V. S. Zotev, A. N. Matlachov, P. L. Volegov, H. J. Sandin, M. A. Espy, J. C. Mosher, A. V. Urbaitis, S. G. Newman, and R. H. Kraus, "Multi-channel squid system for meg and ultra-low-field mri," *IEEE Transactions on Applied Superconductivity*, vol. 17, no. 2, pp. 839–842, 2007.

[15] M. V. Romalis and H. B. Dang, "Atomic magnetometers for materials characterization," *Materials Today*, vol. 14, no. 6, pp. 258–262, 2011.

[16] T. H. Sander, J. Preusser, R. Mhaskar, J. Kitching, L. Trahms, and S. Knappe, "Magnetoencephalography with a chip-scale atomic magnetometer," *Biomedical Optics Express*, vol. 3, no. 5, p. 981, 2012.

[17] O. Alem, T. H. Sander, R. Mhaskar, J. Leblanc, H. Eswaran, U. Steinhoff, Y. Okada, J. Kitching, L. Trahms, and S. Knappe, "Fetal magnetocardiography measurements with an array of microfabricated optically pumped magnetometers." *Physics in Medicine & Biology*, vol. 60, no. 12, pp. 4797–4811, 2015.

[18] D. Budker and M. Romalis, "Optical magnetometry," *Nature Physics*, vol. 3, no. 4, p. 227, 2007.

[19] H. B. Dang, A. C. Maloof, and M. V. Romalis, "Ultrahigh sensitivity magnetic field and magnetization measurements with an atomic magnetometer," *Applied Physics Letters*, vol. 97, no. 15, p. 151110, 2010.

[20] R. Wyllie, M. Kauer, G. S. Smetana, R. T. Wakai, and T. G. Walker, "Magnetocardiography with a modular spin exchange relaxation free atomic magnetometer array," *Physics in Medicine & Biology*, vol. 57, no. 9, p. 2619, 2012.

[21] I. M. Savukov, "Spin exchange relaxation free (serf) magnetometers," in *High Sensitivity Magnetometers*. Springer, 2017, pp. 451–491.

[22] V. Shah and M. V. Romalis, "Spin-exchange-relaxation-free magnetometry using elliptically-polarized light," *Physical Review A*, vol. 80, no. 1, pp. 2460–2462, 2009.

[23] H. G. Dehmelt, "Modulation of a light beam by precessing absorbing atoms," *Physical Review*, vol. 105, no. 6, pp. 1924–1925, 1957.

[24] W. E. Bell and A. L. Bloom, "Optical detection of magnetic resonance in alkali metal vapor," *Physical Review*, vol. 107, no. 6, pp. 1559–1565, 1957.

[25] W. Happer and H. Tang, "Spin-exchange shift and narrowing of magnetic resonance lines in optically pumped alkali vapors," *Physical Review Letters*, vol. 31, no. 31, pp. 273–276, 1973.

[26] W. Happer and A. C. Tam, "Effect of rapid spin exchange on the magnetic-resonance spectrum of alkali vapors," *Physical Review A*, vol. 16, no. 5, pp. 1877–1891, 1977.

[27] Q. Jie, "Experimental research on the principle of serf based atomic ^{129}Xe-Cs spin gyroscope," Ph.D. dissertation,Dept., Beihang University, Beijing, 2012.

[28] K. Kim, S. Begus, H. Xia, S. K. Lee, V. Jazbinsek, Z. Trontelj, and M. V. Romalis, "Multi-channel atomic magnetometer for magnetoencephalography: A configuration study," *Neuroimage*, vol. 89, no. 3, pp. 143–151, 2014.

[29] C. Johnson, P. D. D. Schwindt, and M. Weisend, "Magnetoencephalography with a two-color pump-probe, fiber-coupled atomic magnetometer," *Applied Physics Letters*, vol. 97, no. 24, pp. 413–375, 2010.

[30] V. Shah, S. Knappe, P. D. D. Schwindt, and J. Kitching, "Subpicotesla atomic magnetometry with a microfabricated vapour cell," *Nature Photonics*, vol. 1, no. 11, pp. 649–652, 2007.

[31] W. C. Griffith, S. Knappe, and J. Kitching, "Femtotesla atomic magnetometry in a microfabricated vapor cell," *Optics Express*, vol. 18, no. 26, p. 27167, 2010.

[32] Z. Li, R. T. Wakai, and T. G. Walker, "Parametric modulation of an atomic magnetometer," *Applied Physics Letters*, vol. 89, no. 13, p. 1153, 2006.

[33] M. Ledbetter, I. Savukov, V. Acosta, D. Budker, and M. Romalis, "Spin-exchange-relaxation-free magnetometry with cs vapor," *Physical Review A*, vol. 77, no. 3, p. 033408, 2008.

[34] J. Fang, R. Li, L. Duan, Y. Chen, and Q. Wei, "Study of the operation temperature in the spin-exchange relaxation free magnetometer," *Review of Scientific Instruments*, vol. 86, p. 073116, 2015.

[35] M. P. Ledbetter, I. M. Savukov, D. Budker, V. Shah, S. Knappe, J. Kitching, D. J. Michalak, S. Xu, and A. Pines, "Zero-field remote detection of NMR with a microfabricted atomic magnetometer," *Proceedings of the National Academy of Sciences of the United States of America*, vol. 105, no. 7, p. 2286, 2008.

[36] S. Appelt, B. A. Baranga, C. J. Erickson, M. V. Romalis, A. R. Young, and W. Happer, "Theory of spin-exchange optical pumping of ^{3}He and ^{129}Xe," *Physical Review A*, vol. 58, no. 2, pp. 1412–1439, 1998.

[37] M. V. Romalis, "Hybrid optical pumping of optically dense alkali-metal vapor without quenching gas," *Physical Review Letters*, vol. 105, no. 24, p. 243001, 2010.

[38] Y. Ito, H. Ohnishi, K. Kamada, and T. Kobayashi, "Sensitivity improvement of spin-exchange relaxation free atomic magnetometers by hybrid optical pumping of potassium and rubidium," *IEEE Transactions on Magnetics*, vol. 47, no. 10, pp. 3550–3553, 2011.

[39] Y. Ito, H. Ohnishi, and K. Kamada, "Development of an optically pumped atomic magnetometer using a K-Rb hybrid cell and its application to magnetocardiography," *AIP advances*, vol. 2, no. 3, p. 032127, 2012.

[40] Y. Ito, H. Ohnishi, K. Kamada, and T. Kobayashi, "Effect of spatial homogeneity of spin polarization on magnetic field response of an optically pumped atomic magnetometer using a hybrid cell of K and Rb atoms," *IEEE Transactions on Magnetics*, vol. 48, no. 11, pp. 3715–3718, 2012.

[41] Y. Ito, H. Ohnishi, and K. Kamada, "Rate-equation approach to optimal density ratio of K-Rb hybrid cells for optically pumped atomic magnetometers," in *Engineering in Medicine & Biology Society*, 2013, p. 3254.

[42] J. Fang, T. Wang, H. Zhang, Y. Li, and S. Zou, "Optimizations of spin-exchange relaxation-free magnetometer based on potassium and rubidium hybrid optical pumping," *Review of Scientific Instruments*, vol. 85, no. 12, p. 123104, 2014.

[43] Y. Ito, D. Sato, K. Kamada, and T. Kobayashi, "Optimal densities of alkali metal atoms in an optically pumped K-Rb hybrid atomic magnetometer considering the spatial distribution of spin polarization." *Optics Express*, vol. 24, no. 14, p. 15391, 2016.

[44] P. Schwindt and C. N. Johnson, "Atomic magnetometer for human magnetoencephalograpy," *Albuquerque, New Mexico: Sandia National Laboratories*, 2010.

[45] T. W. Kornack, S. J. Smullin, S. K. Lee, and M. V. Romalis, "A low-noise ferrite magnetic shield," *Applied Physics Letters*, vol. 90, no. 22, p. 67, 2007.

[46] I. Wylie, Robert, "The development of a multichannel atomic magnetometer array for fetal magnetocardiography," Ph.D. dissertation,Dept.physics, University of Wisconsin-Madison, Madison,Wisconsin, 2012.

[47] J. Preusser, S. Knappe, J. Kitching, and V. Gerginov, "A microfabricated photonic magnetometer," in *Frequency Control Symposium, 2009 Joint with the 22nd European Frequency and Time forum. IEEE International*. IEEE, 2009, pp. 1180–1182.

[48] I. A. Sulai, R. Wyllie, M. Kauer, G. S. Smetana, R. T. Wakai, and T. G. Walker, "Diffusive suppression of ac-stark shifts in atomic magnetometers," *Optics Letters*, vol. 38, no. 6, pp. 974–6, 2013.

[49] M. Fleischhauer, A. B. Matsko, and M. O. Scully, "Quantum limit of optical magnetometry in the presence of ac-stark shifts," *Physical Review A*, vol. 62, no. 1, p. 013808, 2012.

[50] K. B. Macadam, A. Steinbach, and C. Wieman, "A narrow-band tunable diode laser system with grating feedback, and a saturated absorption spectrometer for cs and rb," *American Journal of Physics*, vol. 60, no. 12, pp. 1098–1111, 1992.

[51] C. Wieman and T. W. Hnsch, "Doppler-free laser polarization spectroscopy," *Physical Review Letters*, vol. 36, no. 20, pp. 1170–1173, 1976.

[52] G. P. T. Lancaster, R. S. Conroy, M. A. Clifford, J. Arlt, and K. Dholakia, "A polarisation spectrometer locked diode laser for trapping cold atoms," *Optics Communications*, vol. 170, no. 1-3, pp. 79–84, 1999.

[53] V. B. Tiwari, S. Singh, S. R. Mishra, H. S. Rawat, and S. C. Mehendale, "Laser frequency stabilization using dopplerfree bipolarization spectroscopy," *Optics Communications*, vol. 263, no. 2, pp. 249–255, 2006.

[54] K. L. Corwin, Z. T. Lu, C. F. Hand, R. J. Epstein, and C. E. Wieman, "Frequency-stabilized diode laser with the zeeman shift in an atomic vapor," *Applied Optics*, vol. 37, no. 15, p. 3295, 1998.

[55] V. V. Yashchuk, D. Budker, and J. R. Davis, "Laser frequency stabilization using linear magneto-optics," *Review of Scientific Instruments*, vol. 71, no. 2, pp. 341–346, 2000.

[56] P. Wanninger and E. C. Valdez, "Diode-laser frequency stabilization based on the resonant faraday effect," *IEEE Photonics Technology Letters*, vol. 4, no. 1, pp. 94–96, 2002.

[57] J. A. Kerckhoff, C. D. Bruzewicz, R. Uhl, and P. K. Majumder, "A frequency stabilization method for diode lasers utilizing low-field faraday polarimetry," *Review of Scientific Instruments*, vol. 76, no. 9, p. 1098, 2005.

[58] G. Wasik, W. Gawlik, J. Zachorowski, and W. Zawadzki, "Laser frequency stabilization by doppler-free magnetic dichroism," *Applied Physics B*, vol. 75, no. 6-7, pp. 613–619, 2002.

[59] C. D. Tran and R. J. Furlan, "Amplitude stabilization of a multiwavelength laser beam by an acousto-optic tunable filter," *Review of Scientific Instruments*, vol. 65, no. 2, pp. 309–314, 1994.
[60] V. I. Balakshy, Y. I. Kuznetsov, S. N. Mantsevich, and N. V. Polikarpova, "Dynamic processes in an acousto-optic laser beam intensity stabilization system," *Optics & Laser Technology*, vol. 62, no. 10, pp. 89–94, 2014.
[61] K. Nakagawa, A. S. Shelkovnikov, T. Katsuda, and M. Ohtsu, "Fast frequency stabilization of a diode-laser-pumped monolithic Nd:YAG laser with an extra-cavity electro-optic modulator," *Optics Communications*, vol. 109, no. 5-6, pp. 446–450, 1994.
[62] J. M. Bueno, "Polarimetry using liquid-crystal variable retarders: theory and calibration," *Journal of Optics A Pure & Applied Optics*, vol. 2, no. 3, pp. 216–222, 2000.
[63] S. J. Seltzer and M. V. Romalis, "Unshielded three-axis vector operation of a spin-exchange-relaxation-free atomic magnetometer," *Applied Physics Letters*, vol. 85, no. 20, pp. 4804–4806, 2004.
[64] D. Sheng, S. Li, N. Dural, and M. V. Romalis, "Subfemtotesla scalar atomic magnetometry using multipass cells." *Physical Review Letters*, vol. 110, no. 16, p. 160802, 2013.
[65] T. W. Kornack and M. V. Romalis, "Dynamics of two overlapping spin ensembles interacting by spin exchange," *Physical Review Letters*, vol. 89, no. 25, p. 253002, 2002.
[66] G. Vasilakis, J. M. Brown, T. W. Kornack, and M. V. Romalis, "Limits on new long range nuclear spin-dependent forces set with a k-^{3}He comagnetometer," *Physical Review Letters*, vol. 103, no. 26, p. 261801, 2009.
[67] Y. Hu, X. Liu, Y. Li, and M. Ding, "An electro-optic modulator detection method in all optical atomic magnetometer," in *Asia-Pacific Optical Sensors Conference*. Optical Society of America, 2016, pp. Tu3A–6.
[68] T. Karaulanov, I. Savukov, and Y. J. Kim, "Spin-exchange relaxation-free magnetometer with nearly parallel pump and probe beams," *Measurement Science & Technology*, vol. 27, no. 5, p. 055002, 2016.
[69] s. Li, Y. Xu, Z. Wang, Y. Liu, and Q. Lin, "Experimental investigation on a highly sensitive atomic magnetometer," *CHIN. PHYS. LETT.:in English*, vol. 26, no. 6, pp. 276–278, 2009.
[70] H. Huang, H. Dong, L. Chen, and Y. Gao, "Single-beam three-axis atomic magnetometer," *Applied Physics Letters*, vol. 109, no. 6, pp. 227–234, 2016.
[71] J. Fang, S. Wan, J. Qin, C. Zhang, and W. Quan, "Spin-exchange relaxation-free magnetic gradiometer with dual-beam and closed-loop faraday modulation," *Josa B*, vol. 31, no. 3, pp. 512–516, 2014.
[72] S. Li, P. Vachaspati, D. Sheng, N. Dural, and M. V. Romalis, "Optical rotation in excess of 100 rad generated by Rb vapor in a multipass cell," *Physical Review A*, vol. 84, no. 6, pp. 242–245, 2011.
[73] J. Shi, S. Ikalainen, J. Vaara, and M. V. Romalis, "Observation of optical chemical shift by precision nuclear spin optical rotation measurements and calculations," *Journal of Physical Chemistry Letters*, vol. 4, no. 3, pp. 437–441, 2013.
[74] S. Kuriki, A. Hayashi, T. Washio, and M. Fujita, "Active compensation in combination with weak passive shielding for magnetocardiographic measurements," *Review of Scientific Instruments*, vol. 73, no. 2, pp. 440–445, 2002.
[75] J. Fang and J. Qin, "In situ triaxial magnetic field compensation for the spin-exchange-relaxation-free atomic magnetometer," *Review of Scientific Instruments*, vol. 83, no. 10, p. 227, 2012.
[76] J. Fang, T. Wang, W. Quan, H. Yuan, H. Zhang, Y. Li, and S. Zou, "In situ magnetic compensation for potassium spin-exchange relaxation-free magnetometer considering probe beam pumping effect," *Review of Scientific Instruments*, vol. 85, no. 6, p. 596, 2014.
[77] S. K. Lee and M. V. Romalis, "Calculation of magnetic field noise from high-permeability magnetic shields and conducting objects with simple geometry," *Journal of Applied Physics*, vol. 103, no. 8, pp. 67–190, 2008.
[78] J. M. Brown, "A new limit on lorentz-and cpt-violating neutron spin interactions using a potassium-helium comagnetometer," Ph.D. dissertation,Dept.physics, Princeton University, Princeton,New Jersey, 2011.
[79] P. H. Chu, Y. J. Kim, and I. M. Savukov, "Search for exotic spin-dependent interactions with a spin-exchange relaxation-free magnetometer," *Physical Review D*, vol. 94, no. 3, p. 036002, 2016.
[80] W. Quan, Y. Li, and B. Liu, "Simultaneous measurement of magnetic field and inertia based on hybrid optical pumping," *EPL (Europhysics Letters)*, vol. 110, no. 6, p. 60002, 2015.
[81] T. W. Kornack and M. V. Romalis, "Dynamics of two overlapping spin ensembles interacting by spin exchange," *Physical Review Letters*, vol. 89, no. 25, p. 253002, 2002.
[82] T. W. Kornack, "A test of cpt and lorentz symmetry using a potassium-helium-3 co-magnetometer," Ph.D.dissertation,Dept.astrophysical sciences, Princeton University, Princeton,New Jersey, 2005.
[83] F. Allmendinger, W. Heil, S. Karpuk, W. Kilian, A. Scharth, U. Schmidt, A. Schnabel, Y. Sobolev, and K. Tullney, "New limit on lorentz-invariance- and *cpt*-violating neutron spin interactions using a free-spin-precession ^{3}He-^{129}Xe comagnetometer," *Physical Review Letters*, vol. 112, p. 110801, 2014.
[84] J. M. Brown, S. J. Smullin, T. W. Kornack, and M. V. Romalis, "New limit on lorentz-and cpt-violating neutron spin interactions," *Physical Review Letters*, vol. 105, no. 15, p. 151604, 2010.
[85] M. Smiciklas, J. M. Brown, L. W. Cheuk, S. J. Smullin, and M. V. Romalis, "New test of local lorentz invariance using a ^{21}Ne-Rb-K comagnetometer," *Physical Review Letters*, vol. 107, p. 171604, 2011.
[86] G. Vasilakis, "Precision measurements of spin interactions with high density atomic vapors," *Dissertations & Theses - Gradworks*, 2011.
[87] H. Xia, A. Ben-Amar Baranga, D. Hoffman, and M. V. Romalis, "Magnetoencephalography with an atomic magnetometer," *Applied Physics Letters*, vol. 89, no. 21, p. 664, 2006.
[88] C. Johnson, N. L. Adolphi, K. L. Butler, D. M. Lovato, R. Larson, P. D. D. Schwindt, and E. R. Flynn, "Magnetic relaxometry with an atomic magnetometer and squid sensors on targeted cancer cells," *Journal of Magnetism & Magnetic Materials*, vol. 324, no. 17, 2012.
[89] C. N. Johnson, P. D. Schwindt, and M. Weisend, "Multi-sensor magnetoencephalography with atomic magnetometers." *Physics in Medicine & Biology*, vol. 58, no. 17, pp. 6065–77, 2013.
[90] A. P. Colombo, T. R. Carter, A. Borna, Y. Y. Jau, C. N. Johnson, A. L. Dagel, and P. D. Schwindt, "Four-channel optically pumped atomic magnetometer for magnetoencephalography," *Optics Express*, vol. 24, no. 14, pp. 15 403–15 416, 2016.

Jundi Li received the M.S. degree from Beihang University, Beijing, China, in 2012. During 2012-2014, she was a junior engineer with the China helicopter Design Institute, Jiangxi, China.

Currently, she is pursuing her PHD degree in currently working toward the Ph.D. degree at the school of Instrumentation Science and Optoelectronics Engineering, Beijing University of Aeronautics and Astronautics. Her main research interests involve design of magnetic shield system, inertial and magnetic measurements and atomic magnetometer.

Wei Quan received the Ph.D. degree of precision instrument and mechanics in 2008 from Beihang University. As a Professor, he is now working in School of Instrumentation Science and Optical Engineering, Beihang University China. His current research interests are atomic spin inertial measurement, atomic magnetic field measurement, and information fusion navigation et al.

Binquan Zhou was born in 1981 in Shanxi, China. He received the Ph.D. degree of precision instrument and mechanics in 2017 from Beihang University. He is currently an assistant professor at the School of Instrumentation Science and Optical Engineering, Beihang University. He has undertaken multiple national and ministerial research projects including National Natural Science Fund, 863 of Ministry of Science and Technology and so on. His research interests are atomic gyroscope, atomic magnetometer and MEG research.

Zhuo Wang was born in Handan, Hebei Province, China, in 1983. He received the B.E. degree in automation from Beihang University, Beijing, China, in 2006; and the Ph.D. degree in electrical and computer engineering from University of Illinois at Chicago, Chicago, Illinois, USA, in 2013. He was a Postdoctoral Fellow with the Department of Electrical and Computer Engineering, University of Alberta, from 2013 to 2014. He worked as a Research Assistant Professor with the Fok Ying Tung Graduate School, Hong Kong University of Science and Technology, from 2014 to 2015. He was selected for the "12th Recruitment Program for Young Professionals" by the Organization Department of the CPC Central Committee, and the "100 Talents Program" by Beihang University, in 2015. He is currently a Professor and a Ph.D. Instructor with the School of Instrumentation Science and Optoelectronics Engineering, Beihang University, Beijing, China.

Prof. Wang is a Member of the Adaptive Dynamic Programming and Reinforcement Learning Technical Committee of IEEE Computational Intelligence Society, a Member of the Data Driven Control, Learning & Optimization Professional Committee of CAA, and is a Member of the Fault Diagnosis & Safety for Technical Processes Professional Committee of CAA. He is an Associate Editor of IEEE Transactions on Systems, Man, and Cybernetics: Systems, an Associate Editor of Control Theory & Applications, and is an Associate Editor of Pattern Recognition and Artificial Intelligence.

Jixi Lu received the Ph.D. degree in measurement technology and instruments from Beihang University, Beijing, China, in 2016. He is currently a Postdoctor in School of Physics and Nuclear Energy Engineering, Beihang University, Beijing, China. His research interests include atomic magnetometer and electronic-optical detection technology.

Zhaohui Hu received his PhD degree of optical engineering in 2006 from Tsinghua University, China, where he researched as postdoctoral fellow until 2009. He currently works in School of Instrumentation Science and Optical Engineering, Beihang University. His current research interests are atomic magnetometry, atomic gyroscopy, optical pumping, and optical measurement.

Gang Liu was born in Shandong, China, in 1970. He received the B.S. and M.S. degrees in electrical engineering from Shandong University of Technology, Jinan, China, in 1992 and 1998, respectively, and the Ph.D. degree in control engineering from Dalian University of Technology, Dalian, China, in 2001. He is currently a Ph.D. Supervisor in the School of Instrument Science and Optoelectronic Engineering, Beijing University of Aeronautics and Astronautics, Beijing, China. His research interests include spacecraft inertia attitude control actuator technology and precision mechanical and electrical control systems.

Jiancheng Fang was born in Shandong, China, in 1965. He received the B.S. degree in electrical engineering from Shandong University of Technology, Jinan, China, in 1983, the M.S. degree in automotive engineering from Xian Jiao Tong University, Xian, China, in 1988, and the Ph.D. degree in mechanical engineering from Southeast University, Nanjing, China, in 1996.

He is currently the Vice President of Beihang University, Beijing, China. He holds a special appointment professorship with the title of Cheung Kong Scholar, which was jointly established by the Ministry of Education of China and the Li Ka Shing Foundation. He has authored or co-authored over 150 papers and four books. His current research interests include the attitude control system technology of spacecraft, novel inertial instrument and equipment technology, inertial navigation, SERF atomic magnetometer and co-magnetometer.